# Applications of Terahertz (THz) Technology to Medical Imaging

DD Arnone, CM Ciesla, A Corchia, S Egusa, and M Pepper
*Toshiba Research Europe Ltd., Cambridge Research Laboratory, 260 Science Park, Milton Road, Cambridge CB4 4WE U.K*

JM Chamberlain, C Bezant
*Department of Physics , University of Nottingham, Nottingham NG7 2RD U.K.*

EH Linfield
*Department of Physics , Cavendish Laboratory, University of Cambridge, Cambridge NG7 2RD U.K*

R Clothier, N Khammo
*Queens Medical Centre, University of Nottingham, NG7 2RD U.K.*

## ABSTRACT

An imaging system has been developed based on pulses of Terahertz (THz) radiation generated and detected using all-optical effects accessed by irradiating semiconductors with ultrafast (fs-ps) pulses of visible laser light. This technique, commonly referred to as T-Ray Imaging or THz Pulse Imaging (TPI), holds enormous promise for certain aspects of medical imaging. We have conducted an initial survey of possible medical applications of TPI and demonstrated that TPI images show good contrast between different animal tissue types (muscle, fat, kidney, skin, cartilage). Moreover, the diagnostic power of TPI has been elucidated by the spectra available at each pixel in the image, which are markedly different for the different tissue types. This suggests that the spectral information inherent in TPI might be used to identify the type of soft and hard tissue at each pixel in an image and provide other diagnostic information not afforded by conventional imaging techniques. Preliminary TPI studies of pork skin show that 3D tomographic imaging of the skin surface and thickness is possible, and data from experiments on models of the human dermis are presented which demonstrate that different constituents of skin have different refractive indices. Lastly, we present the first THz image of human tissue, namely an extracted tooth. The time of flight of THz pulses through the tooth allows the thickness of the enamel to be determined, and is used to create an image showing the enamel and dentine regions. Absorption of THz pulses in the tooth allows the pulp cavity region to be identified. Initial evidence strongly suggests that TPI may be used to provide valuable diagnostic information pertaining to the enamel, dentine, and the pulp cavity.

Keywords: THz imaging, THz spectroscopy, medical imaging, tooth, skin

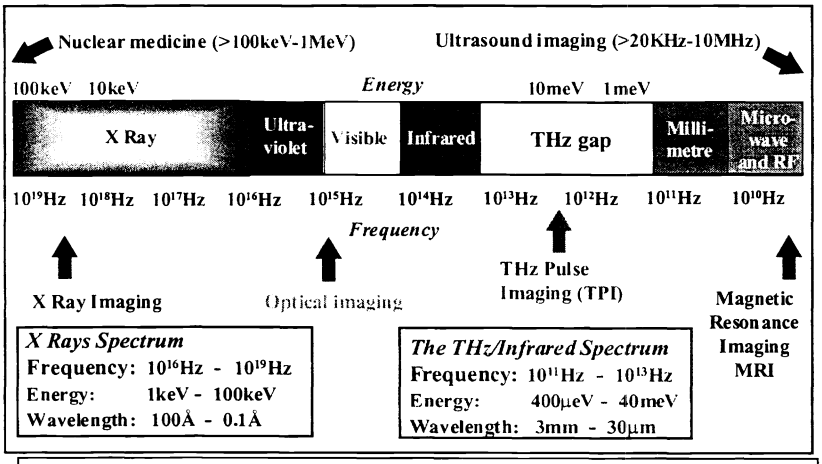


**Figure 1. Medical Imaging and the Electromagnetic Spectrum.**

## 1. TPI VERSUS CONVENTIONAL MEDICAL IMAGING TECHNOLOGIES

In the thirty odd years since the first appearance of coherent light, lasers have become almost commonplace. However, there remains one region of the electromagnetic spectrum - the so-called 'Terahertz Gap' - where bright, coherent sources of radiation do not exist (Fig. 1). Terahertz (THz) typically includes frequencies between 0.1THz to 20THz, where 1THz=$10^{12}$Hz, or in units of wavelength $\lambda$=3mm to 15μm. Over the last decade, advances in ultrafast pulsed visible and near-infrared lasers have lead to coherent generation and detection of sub-

Part of the EUROPTO Conference on Terahertz Spectroscopy and Applications II
Munich, Germany • June 1999 SPIE Vol. 3828 • 0277-786X/99/$10.00

picosecond, broadband (0.05THz-10sTHz) pulses using commercially available technology. Recently, a new imaging technique has been developed based on pulses of THz radiation generated and detected using photoconductive[1] or electro-optical[2] effects with visible pulses (fs-ps) from Ti:Sapphire lasers. This technique commonly referred to as T-Ray Imaging or THz Pulse Imaging (TPI) holds enormous promise for a wide variety of applications. One area of potentially great significance is the application of TPI to medical imaging. Traditional techniques such as X-Ray radiography and computed tomography (CT), magnetic resonance imaging (MRI), ultrasound, and radioisotope imaging are capable of penetrating deep into the body and providing detailed images which represent many years of effort by the medical imaging community. As competition with such accomplishments would be difficult at this early stage of development, applications of TPI should focus initially on specific areas where THz light might have imaging and diagnostic capabilities not afforded by the conventional imaging techniques, such as the potential ability of TPI to distinguish between certain types of healthy and abnormal soft tissue. Its penetration depth for various tissue types, as well as its ability to distinguish between different tissue types, will therefore dictate the utility of THz in medical investigations. The ultimate goal of TPI is to provide high quality images that contain diagnostic information not readily available with other techniques. TPI could provide such information for certain medical applications where it might have distinct advantages over X-Ray, MRI, and ultrasound because of a) its possible diagnostic capabilities arising from the spectral information available at each pixel in the image, and also due to b) the *multiplicity of contrast mechanisms available in TPI.* At each pixel in an image, one can plot:

1. The absorption coefficient $\alpha(\omega)$ over the entire frequency bandwidth of the THz pulse: *panchromatic absorption image,*
2. The absorption coefficient $\alpha(\omega)$ at a fixed frequency $\omega$ or over a limited frequency range covered by the THz pulse: *monochromatic absorption image,*
3. Thickness of the object: *time-of-flight image*, or
4. Refractive index $n(\omega)$ at a fixed frequency or over the entire bandwidth: *refractive index image.*

We illustrate these unique and powerful attributes of TPI below in a series of examples relevant to medical imaging.

## 2. DESCRIPTION OF TPI

### 2.1. Fundamentals and Description of Current System

A TPI system based on difference frequency generation of THz pulses (bandwidth ~ 0.3THz-2.7THz) and electro-optic detection via the ac Pockels effect[2] has been developed at the Cambridge Research Laboratory (CRL) of Toshiba Research Europe Ltd. (TREL) (Fig. 2). Generation of THz pulses is based on difference frequency mixing arising from the second order susceptibility $\chi^{(2)}$ of a semiconductor crystal (here <110> ZnTe). Ultrafast red ($\lambda_{vis}$ =800nm) visible pulses with a temporal width of ~70fs have a frequency bandwidth in excess of 10THz. Exciting a crystal having large $\chi^{(2)}$ with such an ultrafast visible pulse produces a time-dependent polarisation where the different visible frequencies beat against each other to create a polarisation $P_{NL}$ at the difference frequency, $\omega_{THz}$:

$$P_{NL}(\omega_{THz})=\chi^{(2)}E(\omega_{vis1})E(\omega_{vis2}), \quad (1)$$

where $\omega_{THz}=|\omega_{vis1}-\omega_{vis2}|$, and $\omega_{THz}$, $\omega_{vis1}$, $\omega_{vis2}$ are the THz and visible frequencies, respectively. This time varying polarisation emits a pulse of THz electromagnetic radiation that contains a broad range of frequencies from dc up to the bandwidth of the visible radiation.

Conventional detectors for THz radiation rely on liquid helium cooled bolometers, which measure only the intensity of the radiation, have a background limited sensitivity, and do not provide any phase information. Using mechanisms that are similar to those responsible for the generation of broadband THz pulses, it is now possible to directly and coherently measure the THz electric field in the time domain with high sensitivity at room temperature, without any requirement for cooling

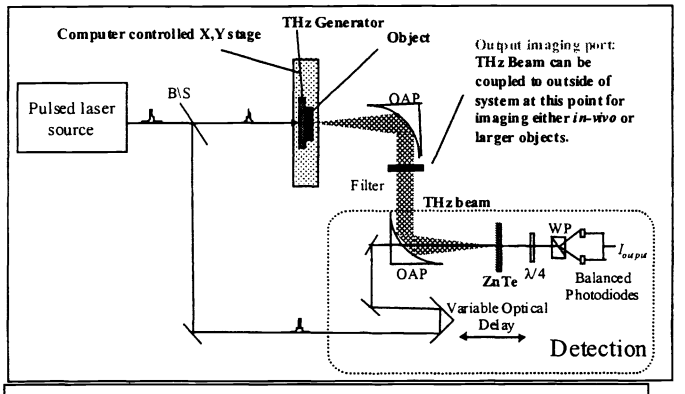


**Figure 2. TPI Imaging Platform. The Entire System is Controlled by a DeskTop PC. Further Explanation of Symbols in Text.**

of components. The technique being used at TREL-CRL uses the linear electro-optical effect known as the ac Pockels effect[2]. A THz pulse incident on an electro-optical medium (again <110> ZnTe) induces birefringence that is proportional to the amplitude of the THz electric field. This birefringence is readily probed using a visible (probe) beam that experiences a retardation on propagation through an electro-optic medium that is measured with inexpensive and commercially available visible wavelength components and photodetectors. Due to the instantaneous response of the electro-optical material, electro-optical sampling (EOS) in principle has an extremely high bandwidth with a flat frequency response, and allows a direct measurement of the amplitude, phase and spatial distribution of the THz electric field.

The system is shown schematically in Fig. 2. The main components of the system are (a) femtosecond (fs)-pulsed visible laser, (b) THz generator, (c) coupling optics for the THz beam, and (d) time-resolved EOS measurement of the THz pulses. The visible laser source is a commercial ultrafast pulsed Ti:Sapphire oscillator pumped by a diode laser-driven cw solid state laser. The Ti:Sapphire oscillator is tunable over the 750-890nm range, producing short pulses down to 50fs, with a maximum power of ~1W. The visible beam is split in to two equal parts by a beam-splitter (B/S); one part of the beam is used for generating the THz and the other portion is used for detection. The THz is generated using difference frequency mixing in a semiconductor by focussing the visible beam to a 250μm diameter spot using a concave mirror ($f$=250mm, not shown in Fig. 2). We have found that for optimum generation of THz using difference frequency mixing, the semiconductor is mounted normal to the visible beam, with an adjustment for the azimuthal angle in order to maximise $\chi^{(2)}$. In this geometry the THz is emitted in transmission through the semiconductor and the waist of the visible beam determines the size of the THz source. The emitted THz diverges from this small source, and is collimated by an $f$=30mm off-axis parabolic mirror (OAP).

For the EOS detection, a second OAP ($f$=30mm) focuses the THz beam onto the EOS detection crystal, which is <110> ZnTe for all experiments. <110> ZnTe has a large electro-optic coefficient, thus giving a high detection sensitivity, and is also transparent at $\lambda_{vis}$ =800nm and in the THz, thus permitting a long interaction length between the THz and visible fields. The retardation experienced by the visible pulse arising from the Pockels effect in <110> ZnTe is measured using the combination of a quarter wave-plate (λ/4), a polarisation-splitting (Wollaston (WP)) prism and a balanced photodetector assembly. With no THz field present, the linearly polarised visible (probe) beam passes through the ZnTe with a negligible change in its polarisation. After passing through the quarter wave-plate, the beam polarisation is transformed from linear to circular, and then the Wollaston prism spatially separates the vertical and horizontal components of the polarisation. For a perfectly circularly polarised beam the components are equal in intensity. The two beams are detected using a balanced photodiode pair, where the output current is equal to the difference in the photocurrents from the two diodes. In the presence of a THz signal, the change in the ZnTe refractive index retards the probe beam, changing the polarisation state from linear to elliptical. Thus, the intensities of the vertical and horizontal beams following the Wollaston prism are no longer equal, and a non-zero photocurrent is measured. Due to the linear shift of the ZnTe refractive index with THz electric field, the output current is proportional to the magnitude of the THz electric field. Neglecting propagation effects in the ZnTe and assuming a delta function-like probe pulse, the instantaneous response of the Pockels effect allows the THz electric field to measured in the time domain simply by varying the arrival time of the THz and probe pulses at the ZnTe detector. This is achieved using a mirror mounted on a computer-controlled delay

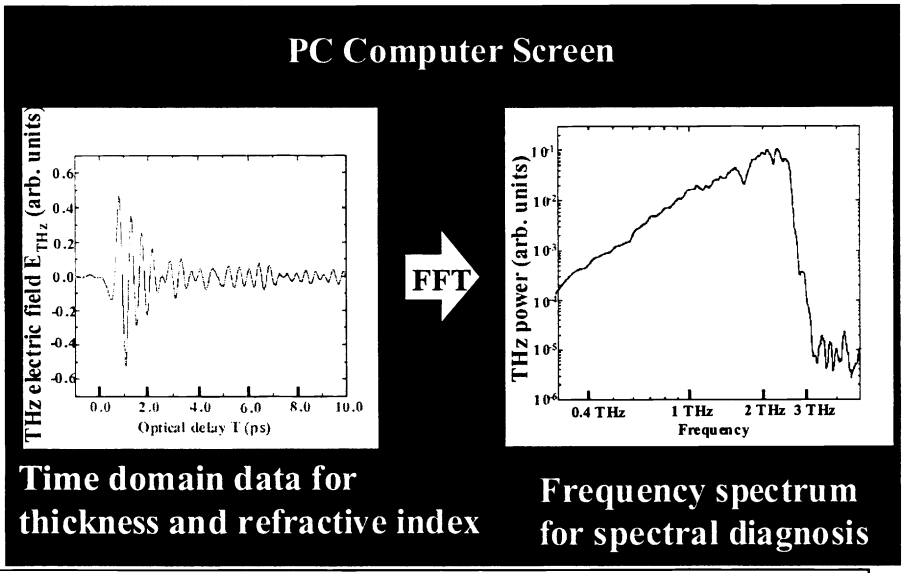


**Figure 3. Time and Frequency Domain Data Available at Each Pixel in TPI Image.**

stage; moving the mirror back increases the probe path length, and thus delays the arrival of the visible pulse at the ZnTe, allowing the THz pulse waveform to be measured at a later time.

Mounting the object on the rear of the generation crystal, and stepping both the object and the generation crystal through the visible generation beam performs imaging. An X-Y translation stage (see Fig. 2) allows THz spectra to be recorded at each pixel in the image (see Fig. 3). Time domain data is displayed on the PC computer screen, or frequency domain data may be examined at each pixel in the image by applying a fast Fourier transform to the time domain data. *This ability to provide the THz spectral fingerprint of the object at each pixel in its image is one of the major advantages of TPI relative to X-Ray, MRI, and other conventional imaging technologies.* Spatial resolution of 200μm is common in the TREL TPI system illustrated here, limited by diffraction in the far field. Better resolution may be achieved by near field imaging of thin objects (several hundred μm thick and located several hundred μm from the generation crystal); near field imaging is not diffraction limited, and spatial resolution is dictated largely by the diameter of the visible beam in the generation crystal, which can be made 50μm or less.

### 2.2. TPI System Development

For imaging of larger objects or those that are not easily accessible or easily mounted on the generation crystal, more sophisticated THz and/or visible optics may be used to couple THz into and out of the object under study. In this way, it will be possible to perform TPI on a wide variety of objects, large and small, *in vivo*. In addition, the system in Fig. 2 can be made more compact and durable in a variety of ways using new innovations. A significant part of our current work focuses on developing such systems for the future. We are also concerned with design and fabrication of new semiconductors for much larger visible to THz conversion efficiency, which will produce higher THz power levels and enable us to penetrate through thicker objects. Similar effort is being devoted to new detection schemes to improve signal- to-noise ratios and hence increase image quality and acquisition times.

## 3. CONTRAST IN TPI BETWEEN DIFFERENT SOFT TISSUE TYPES: PANCHROMATIC ABSORPTION IMAGING AND DIAGNOSTIC INFORMATION AT EACH PIXEL

### 3.1. Differentiation Between Tissue Types

As a precursor to the examination of abnormal or diseased tissue, we have investigated contrast in TPI between different types of normal tissue. Initial 2D panchromatic (0.3THz-2.7THz) TPI images of pork samples obtained from a local butcher and containing a variety of different tissue types - muscle, fat, and kidney - are shown in Fig. 4b, along with the corresponding visible photograph of the sample in Fig. 4a. The excellent contrast seen between the different types of tissue in the TPI image, as well as the ability of the relatively low power (average power ~1.1μW, peak energy ~*f*J) THz pulses to pass through these different tissue types (typically 2mm in thickness) are very encouraging for future medical applications. These images were obtained by plotting the peak THz electric field of the transmitted pulse (Fig. 5a) as a function of X-Y position on the sample. Fourier transforming the time domain data leads to the spectral plots of transmission vs. frequency such as that in Fig. 5b, which may be obtained for each pixel in the image. Fig. 5b demonstrates that variations in absorption (transmission) occur across the THz range for each of the tissue types imaged. Moreover, the spectra for different tissue types are markedly different across the THz range probed, allowing the tissue type to also be identified from the absorption spectra. Similar differences in the THz spectra of thin chicken muscle, skin, and cartilage have also been measured (Fig. 6). *This work suggests that different soft tissue types may have characteristic spectral fingerprints in the THz range.* Besides the diagnostic information that may be contained in these spectra, the differences in absorption at a given THz frequency yield monochromatic images at different frequencies that

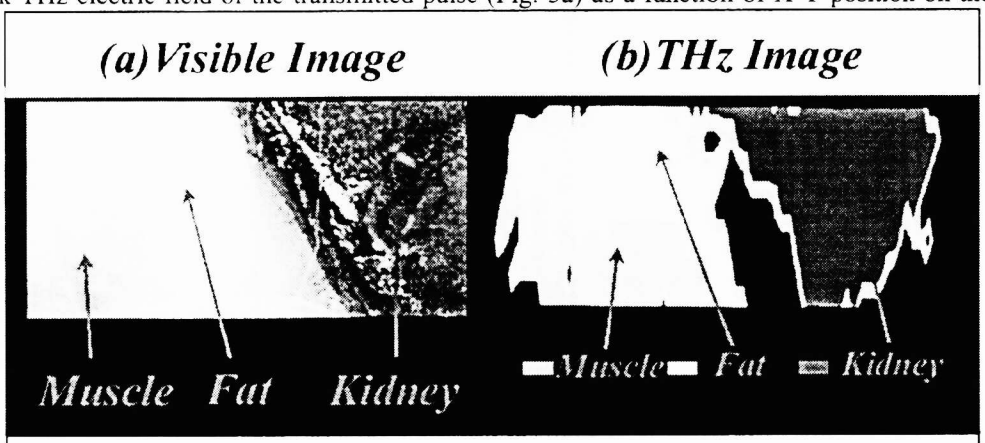


**Figure 4. Visible (a) and THz (b) Images of Different Soft Tissue Types in Pork Sample.**

allow the operator to optimise the contrast between different soft tissue types. However, this preliminary work should be qualified by the fact that the samples were partially dry due to the nature of these initial measurements. The ability to distinguish between different types soft tissue types, suggested by the data above, may lead after further development work to the use of TPI in certain medical applications where the imaging of abnormal or diseased tissue is not adequate using X-Rays or financially feasible using MRI.

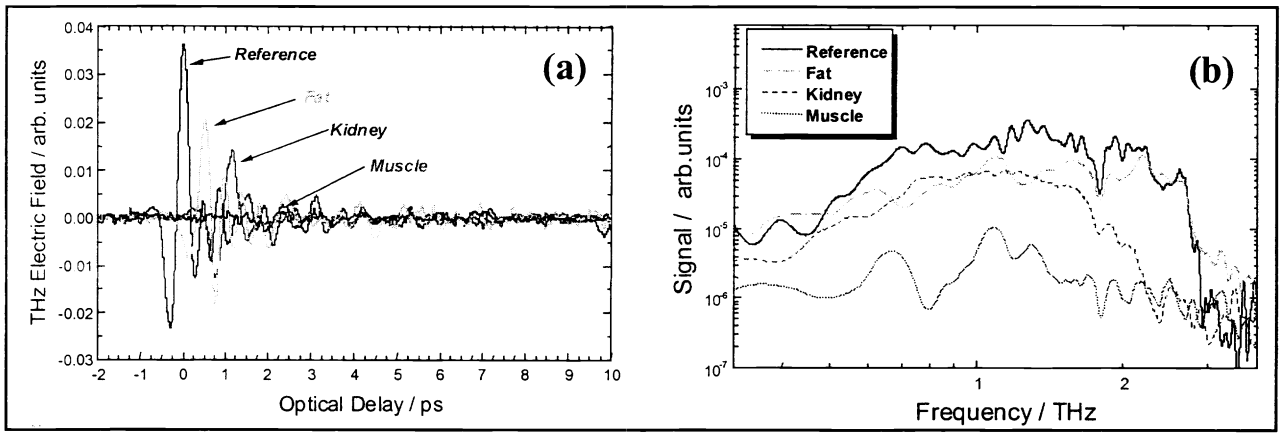


**Figure 5. (a) Time Domain Data Used to Produce Panchromatic Image of Soft Tissues, and (b) THz Spectral Fingerprints of Different Soft Tissues for Thin Pork Sample.**

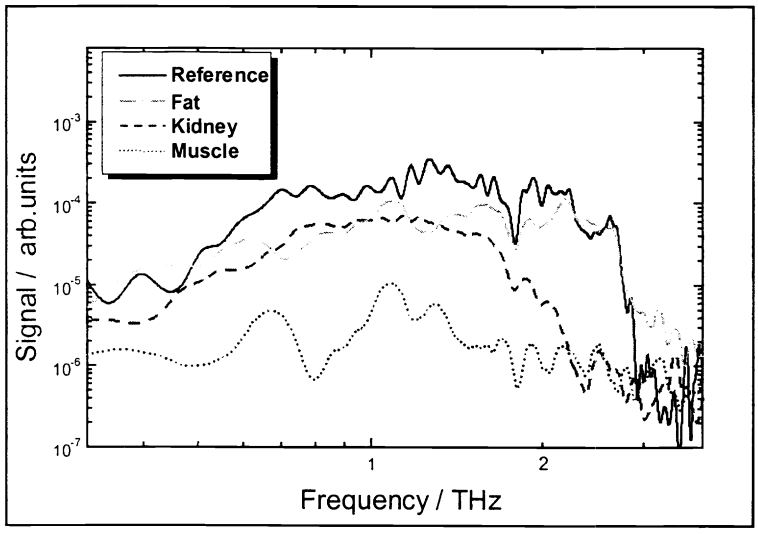


**Figure 6. THz Spectral Fingerprints of Different Tissues for Chicken Sample.**

### 3.2. Preliminary Studies of Model Dermis Systems

Current work is addressing the issue of differentiation between various types of fully moisturized tissue. Preliminary work (Fig. 7) on model dermis systems[3] stored in bovine calf serum and recorded several hours after removal from an incubator suggests that THz radiation readily penetrates such samples with 0.5-1.5mm thickness, despite the low average power levels used (1μW). Moreover, excellent reproducibility is observed between two nominally identical dermis samples (Fig. 7). In addition, the refractive indices of various tissue types and substances can be reconstructed from the time delay of the pulse as it travels more slowly through the tissue relative to air (Fig. 8). Preliminary work (Fig. 8) suggests that the refractive indices of the serum (~3.9), dermis with serum (1.4), and water (~2.2) all differ in the 0.3THz-2.7THz range. It should therefore be possible to determine a tissue type not only from its absorption of THz light, but additionally from its refractive index n(ω) which can also be extracted from TPI. Besides this useful diagnostic information, variation in n(ω) between different tissue types is also the basis of yet another image contrast mechanism in TPI (see Eq. (2) below).

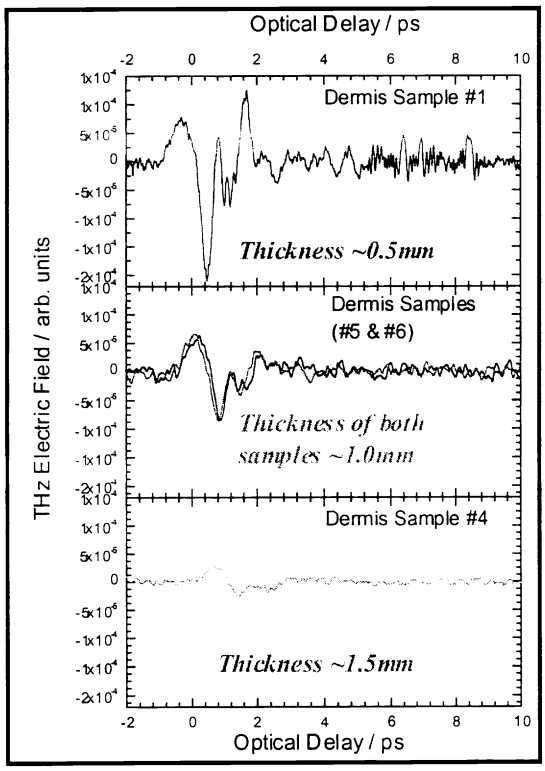


**Figure 7. THz Transmission Through Different Thickness Model Human Dermis.**

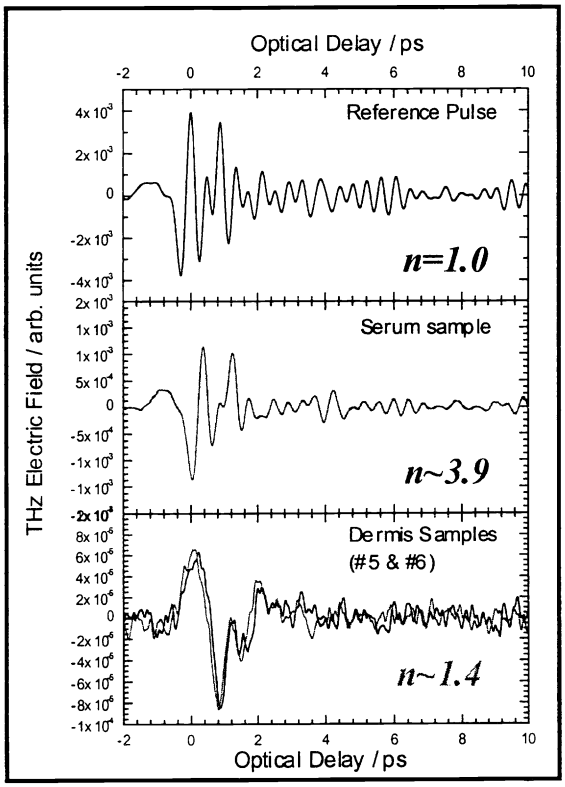


**Figure 8. THz Transmission through Skin Constituents Including Serum, and Model Dermis in Serum. *n* is the Index of Refraction, Which is Different for the Different Materials.**

## 4. 3D MAPPING OF SKIN THICKNESS USING TPI: TIME-OF-FLIGHT IMAGING

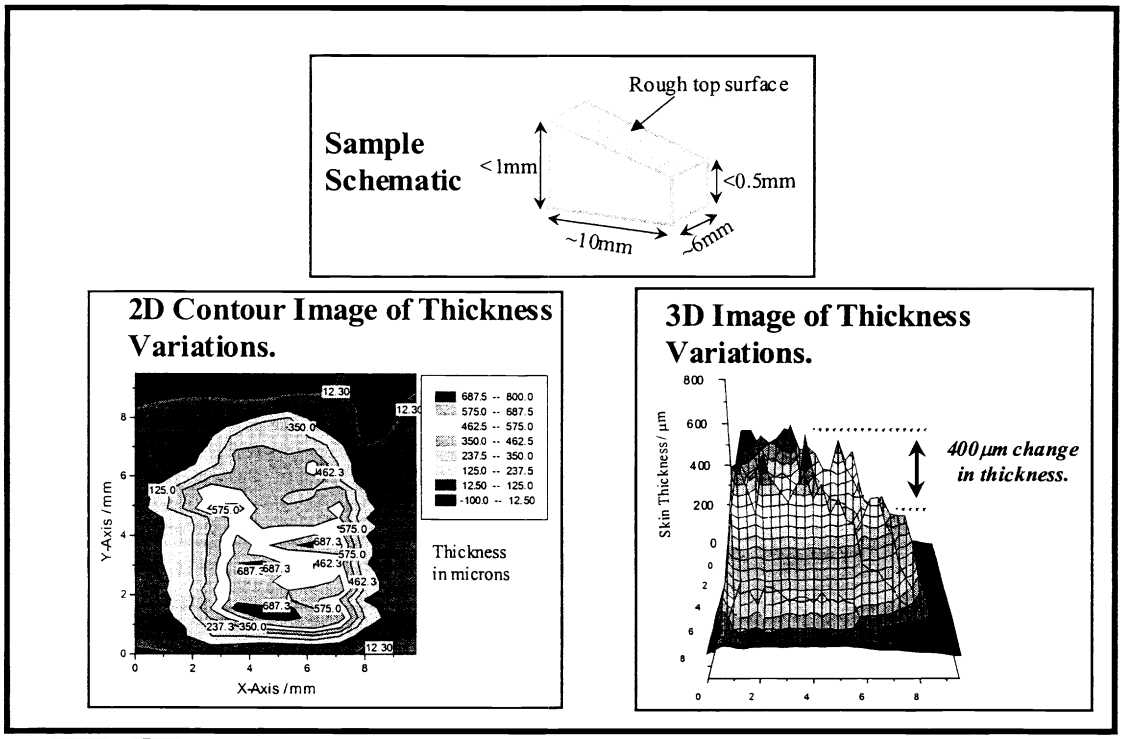


**Figure 9. 3D Tomographic TPI Image of Variations in Skin Thickness Across a Pork Skin Sample.**

Another set of contrast mechanisms available in TPI which further distinguishes it from some of the conventional imaging technologies is the ability to accurately determine (to within <10fs) the time of flight of the THz pulse through an object. The time of flight or delay of a THz pulse through an object of thickness $d$ and refractive index $n$, relative to a reference pulse travelling through air, is given by

$$\text{Delay} = d(n-1)/c. \qquad (2)$$

Hence, by measuring the delay of the THz pulse passing through an object at speed $c/n$ relative to a reference pulse traveling at the speed of light in free space $c$, the thickness $d$ can be determined to an accuracy of typically ±1µm. By plotting the thickness determined from Eq. (2) at each X-Y pixel, a 3D tomographic image of the object thickness can be easily constructed. Fig. 9 shows such an image of a 10mmx6mm area dried pork skin sample that varied in thickness from approximately 1mm at one end to <0.5mm at the other end. In Fig. 9, the sample is depicted schematically along with the 3D TPI transmission image, which faithfully reconstructs the thickness variation in the X-Y plane. Moreover, the thickness variations seen in the image were reproducible, corresponding to changes in thickness on the order of 100-200µm on a length scale of 500µm to 1mm in the X-Y plane. These reproducible variations may be due to hair follicles, but further study of the skin roughness on both faces of the sample is required for confirmation. Similar variations in thickness could be recorded using reflection techniques, which suggests that TPI may prove useful in the imaging of various skin conditions and burn diagnostics, as well as serve as a means of substantiating claims for cosmetic treatments of skin.

## 5. TPI OF HUMAN TISSUE: AN EXTRACTED TOOTH

The obvious, ultimate goal of any medical application of TPI is to serve as an imaging and diagnostic tool on humans. Even at this early stage of development, any data on human tissue that elucidates the advantages and disadvantages of TPI relative to conventional imaging techniques is very useful. We therefore imaged an extracted human tooth. In addition to delivering the first-ever TPI images of human tissue, this preliminary study also provided an excellent demonstration of the power of TPI. In particular, we utilised the different contrast mechanisms available in TPI to construct two very different images containing different types of medically pertinent information. Both of these images were constructed from the same data set.

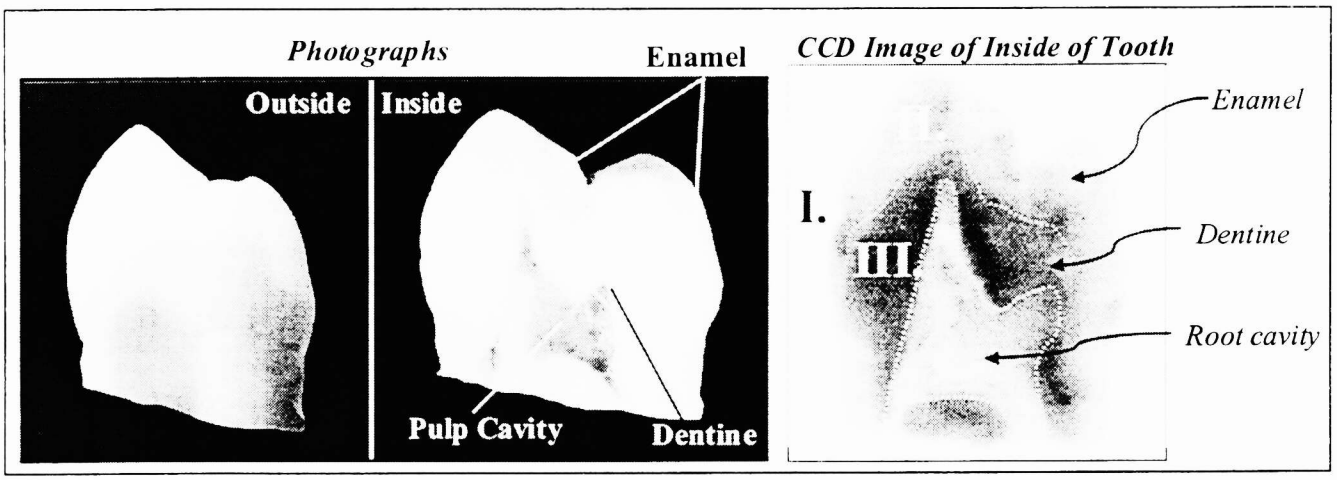


**Figure 10. Visible Photographs of Outside and Inside of the Tooth, Along With Inside View Taken on a CCD Camera to Illustrate Enamel, Dentine, and Root Cavity. Images Inside Were Taken With The Tooth Cut in Half. Regions I., II., and III. are Discussed in the Text.**

The tooth was an extracted premolar. At a frequency of 0.7THz, the absorption coefficient was estimated as $8cm^{-1}$ from a tooth that was roughly 9mm thick. In order to visibly examine the root canal, dentine, and enamel of the tooth, as well as to reduce the data acquisition time of the image, the tooth was cut in half and imaged. Fig. 10 shows external and internal photographs of the tooth, along with a view of the inside of the tooth taken by a CCD camera. The pulp cavity, enamel, and dentine can be seen on the inside photograph, but the CCD image provides even better contrast between these regions. The thickness of the tooth in the X-Y image plane varied from 1mm at one end to 4 mm at the other end.

**5.1 Diagnostic Information on Enamel Thickness and Dentine: Refractive Index Imaging Using Time-of-Flight Data**

Eq. (2) suggests that the changes in the refractive index from one type of tissue to another can result in large changes in the delay or time of flight of the THz pulse through the object under study. This delay or difference in the time of flight can in turn be used to construct an image of the object. To assess whether such a contrast mechanism might be utilised in dental imaging, time domain traces of the THz pulse were recorded in three different regions: I. outside the tooth, II. in the enamel region, and III. in a region covered by both enamel and dentine (see Fig. 10). Moving from outside the tooth (I) to inside the enamel region (II), a large delay (10ps) occurs as the pulse travels through the tooth enamel. As the pulse moves from the enamel region (II) into the immediately adjacent enamel and dentine region (III), a large decrease in the delay is observed (reduction to 5ps) in spite of a very small change in overall tooth thickness. This data suggests a relatively large change in refractive index at THz frequencies between the enamel and dentine. Such a change might be expected. First of all, enamel is harder and therefore is more likely to be denser than dentine, which would increase the refractive index. Accompanying this are important structural differences between enamel and dentine. Moreover, the chemical composition of the two tissues is likely to be different and also result in different indices. Enamel is ~99% mineral, whereas dentine is ~70% mineral. Such different chemical compositions are supported by the different shapes of the pulses, which show that the absorption spectra are very different in between the dentine and enamel in the THz range.

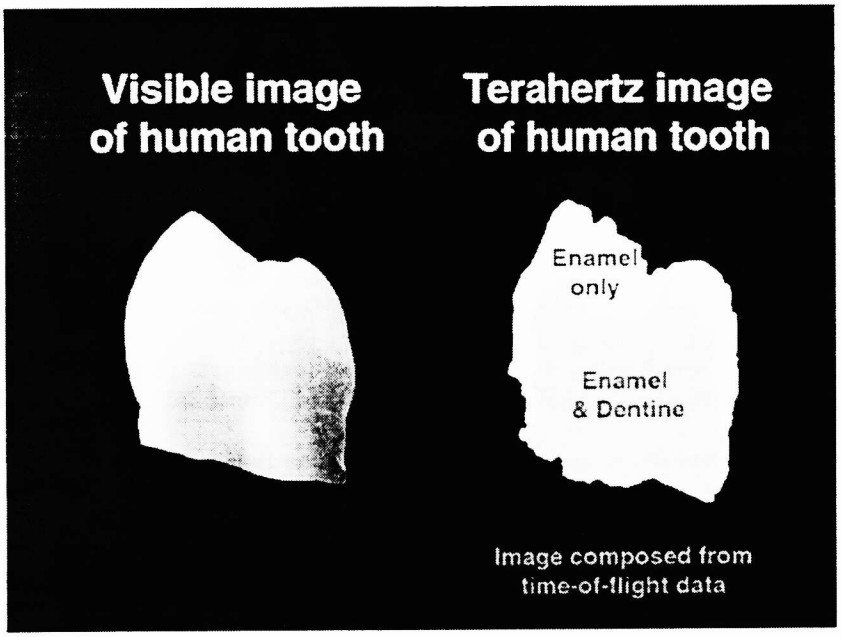


**Figure 11. 2D Contour Plot of THz Pulse Time Delay Data in Figure 14 at Different Pixels (X,Y), Along With Photograph of Tooth.**

All of the time-of-flight data is summarised in Fig.. 11, which shows a 2D contour plot of the data at each pixel. Time-of-flight data in TPI is therefore a convenient means of mapping out regions of enamel, and enamel plus dentine, as well as accurately determining the thickness of these different regions. Additional diagnostic information might be contained in the THz spectra corresponding to the various time domain traces in these different regions.

### 5.2 Diagnostic Information on Pulp Cavity: Panchromatic Absorption Imaging

The same THz data set used to construct the enamel and dentine images above may be manipulated in a different fashion to produce an image of the pulp cavity. Plotting the peak THz electric field of the transmitted pulse (Fig. 12) at each pixel allows us to peer into the pulp cavity. In particular, we note strong absorption in the pulp cavity (Fig. 12) which appears to reflect the build up of additional material in this area. For an empty cavity in an extracted tooth, one would expect the absorption to decrease in the cavity due to an absence of tissue. This preliminary result therefore suggests that the panchromatic absorption contrast mechanism in TPI may provide important diagnostic information about the state of the pulp cavity.

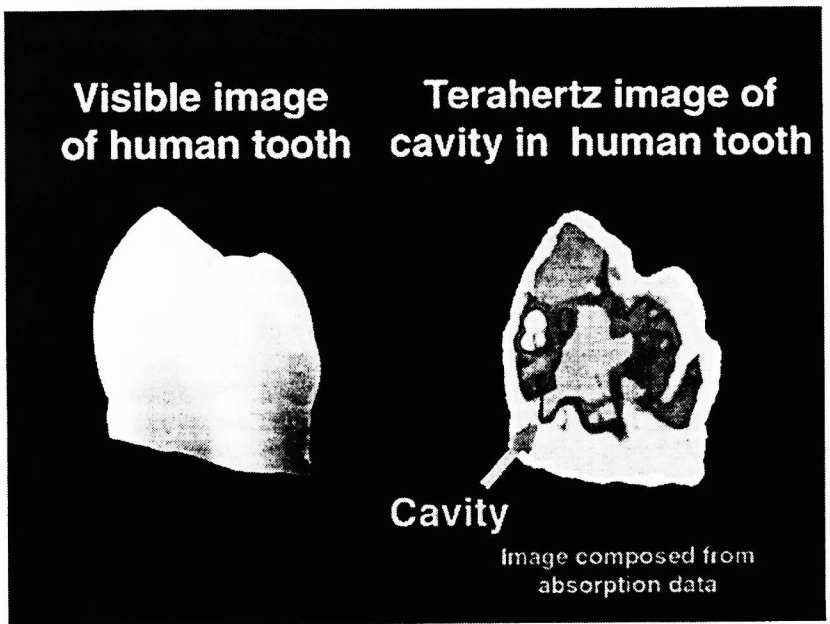


**Figure 12. 2D Contour Plot of THz Transmission Data at Different Pixels (X,Y), Along With Photograph of Tooth.**

*Figs. 11 and 12 illustrate the power of TPI; two very different images providing different information about the tooth can be constructed from the same THz data set.*

## 6. FUTURE PROSPECTS FOR TPI IN MEDICAL IMAGING

### 6.1 Advantages Over Other Imaging Modalities

The preliminary studies of the different types of soft and hard tissue discussed above suggest that TPI may have a bright future in very specific areas of medical imaging. Relative to many conventional techniques, TPI represents a safe, non-invasive, and inexpensive clinical imaging modality with possible added diagnostic abilities. Although conventional imaging techniques such as X-Ray, X-Ray CT, MRI, ultrasound, or radioisotope imaging are currently available and yield impressive results, each has its shortcomings. These can include 1) high cost, 2) low spatial resolution, 3) safety concerns, and 4) limited or non-existent diagnostic capabilities due to lack of specificity to the chemical make-up of tissue. TPI may address some or all of these limitations: 1) lack of magnetic field and expensive X-Ray tubes imply relatively low cost, 2) spatial resolution of 200-500μm is typical for thin (<5mm) tissue, 3) THz radiation is non-ionising and the average power levels currently in use are comparable to the natural background, and the 4) spectral information inherent in TPI (extendable to down into the microwave region and up into the mid-infrared) may relay important pathological and diagnostic information.

TPI also has an important advantage relative to other laser-based imaging techniques such as fluorescence imaging and optical coherence tomography that operate in the near-infrared and visible regions of the spectrum. The development of optical-based imaging modalities has traditionally been hindered by the scattering of light in the tissue at the relatively short wavelengths used in the near-infrared and visible (e.g. λ=400nm-1300nm). The result of this scattering is attenuation of light as well as image blurring. Scattering can significantly alter the directionality, intensity, coherence, polarisation, and pulse width of the radiation probing an object. Whilst recent advances[4] have sought to redress the effects of scattering at these short wavelengths using techniques which manipulate time resolved luminescence or ballistic and snake photons, scattering remains a considerable obstacle in most biomedical applications. For highly scattering or thick media, image bearing light such as ballistic or snake photons become weak. Complicated light patterns around the object must then be measured, and this data modeled with complex computer analysis to reconstruct the image[5]. THz light, by contrast, has very long wavelengths (e.g. λ=15μm-3mm). Because the scattering probability is inversely proportional the fourth power of wavelength, $1/\lambda^4$, significant improvements are expected to rapidly occur in image quality and signal-to-noise ratios as one increases the wavelength. For example, using typical wavelengths of $\lambda_{vis}$ =800nm for optical imaging and $\lambda_{THz}$=150μm for TPI, scattering should be reduced by a factor of over a billion ($1.2x10^9$) in THz imaging and spectroscopy of tissue. This should lead to paradigm shift in the quality of optical images at THz frequencies. Our preliminary work on the human tooth using TPI suggests that this is the case; spatial resolution on the order of 200μm was achieved with no evidence of significant scattering of the THz beam.

### 6.2 Prospects for Overcoming the Limitation on Penetration Depth

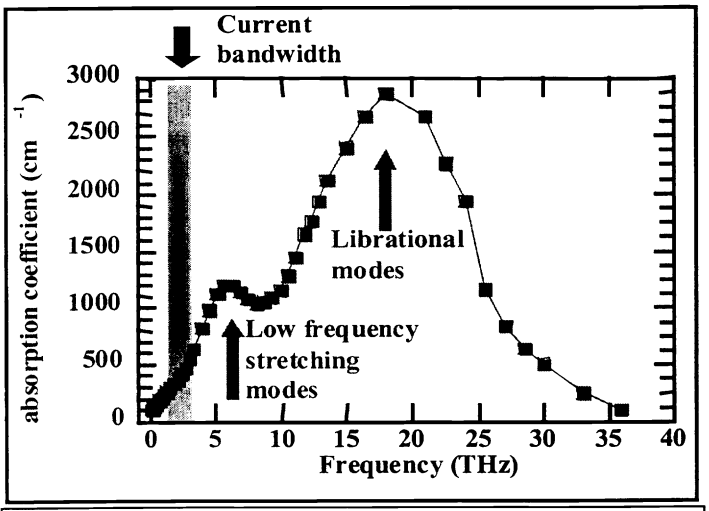


**Figure 13. Water Absorption Coefficient in Millimetre Wave, THz, and Mid-Infrared.**

TPI really suffers from only one significant disadvantage relative to conventional and visible/near-infrared imaging techniques that must be overcome before imaging deep inside the body is feasible. Water has strong and broad librational (19.5THz) and stretching (6THz) absorption modes in the THz range[6]. Absorption is particularly acute toward the high frequency end of the THz region (Fig. 13). Using the 0.3THz-2.7THz bandwidth, 1μW average power, and *f*J pulse energies available from our current TPI system, 2-3mm of moist dermal tissue can be penetrated, similar to typical penetration depths for ballistic photons used in visible and near-infrared imaging. However, the penetration depth for THz can be considerably improved by increasing THz power. Ultimately, the signal-to-noise ratio of a TPI system will determine the useful penetration depth in image acquisition, and therefore any improvement in incident THz power will allow thicker tissue to be examined. For example, preliminary work suggests that increasing the average THz power to the 1mW level will allow up to 8mm of skin to be imaged in the present bandwidth range. Very recent innovations at TREL have further increased the visible to THz conversion efficiency of the semiconductor crystal and allowed us to reach such power levels using conventional, unamplified ultrafast laser

oscillators. These power levels may also be achieved using photoconductive converters, and/or ultrafast regenerative laser amplifiers to boost the visible pulse energy available to pump the semiconductor. Thus, substantial gains in penetration depth will be achieved as THz power levels rise due to advanced engineering of semiconductors for greater visible to THz conversion efficiency, as well as the use of more compact, affordable, and powerful laser regenerative amplifiers.

Fig. 13 also shows that moving down or significantly up in frequency away from our current range (0.3THz-2.7THz) will be beneficial due to reduced water absorption. For example, with our current modest signal to noise ratio of 500:1, approximately 335μm of water can be studied in transmission measurements given our current bandwidth which peaks near 2.0THz. Shifting our coverage down to even 0.3THz would allow penetration through approximately 1mm of water. Similarly, water absorption decreases in the mid-infrared between 30THz and 45THz, as well as 54THz to 90THz, but this absorption is still larger than in the visible and near-infrared between 700nm and 1300nm. EOS detection as described in Section 2.1 has been used to extend coverage to the entire frequency range from 100GHz up to 70THz in a single THz pulse[7]. Combining such techniques with higher powers may provide one possible route to imaging much deeper into the body.

Most importantly, it should be noted that the preliminary indications of our studies suggest that water may not necessarily be as limiting a factor on tissue penetration depth as one might assume. Studies on the moist model human dermis in Section 3.2 suggest that at 2.0THz, the absorption coefficient for a sample is $\alpha \sim 35 cm^{-1}$, implying a penetration depth of 1.8mm for our modest signal-to-noise ratio of 500:1. This agrees well with experiment, where we comfortably went through 1.5mm of dermis without significant noise limitations. By contrast, the absorption coefficient for water near 2.0THz is $\alpha \sim 185 cm^{-1}$, over 5 times larger than that of the dermis. Thus, an analysis based solely on water content would imply that only 334μm of dermis could be penetrated, over 5 times less than found in practice. The limited contribution of water to the absorption coefficient is also demonstrated by the fact that a 2.0THz, $\alpha \sim 35 cm^{-1}$ for moist dermis whereas $\alpha \sim 29 cm^{-1}$ for dry dermis. The 1mW average power levels that are now achievable suggest that ~ 4mm of moist dermis could be probed. Our results in Figs. 5 and 6 (Section 3.1) on animal tissue imply that other tissue types such as fat and cartilage may have even smaller values of $\alpha$ and hence much larger penetration depths. By way of example, tissue with $\alpha = 25 cm^{-1}$ could be probed to depths of 5mm, whereas $\alpha = 3 cm^{-1}$ would allow tissue thickness in excess of 4cm to be imaged. This information points strongly to the need for more comprehensive, systematic, and accurate characterisation of the absorption coefficient $\alpha$ and the refractive index $n$ of a variety of different tissue types at THz frequencies. Such a development programme is needed to pinpoint the areas of medical imaging where TPI will and will not be effective for imaging requiring deep penetration. Married with such efforts should be a continued programme to improve signal-to-noise ratios through more powerful sources and sensitive detectors. Lastly, effort is concentrated on the development of an innovative system for *in-vivo* TPI.

Additional information may be obtained from Dr DD Arnone: email don.arnone@crl.toshiba.co.uk
Website: http://www.toshiba-europe.com/research/index.html
Tel. +44 (0) 1223 424666 Fax +44 (0) 1223 424341

[1] B.B. Hu and M.C. Nuss, *Optics Letters* **20** 1716-1718 (1995).

[2] Q. Wu, T.D. Hewitt, and X.-C. Zhang, *Applied Physics Letters* **69** 1026-1028 (1996).

[3] A model dermis is formed by growing a collagen disk that has in it human fibroblasts that have caused the collagen to cross link and hence condense to form into a disc. The collagen comes from rats, and all growth is carried out in an incubator. The samples are stored in an incubator up to several hours before the experiment in an attempt to keep them 'alive' during the experiment.

[4] P. French, *Physics World* **69** 41-46 (June 1999).

[5] S.K. Gayen and R.R. Alfano, *Optics Express* **4** 475-480 (1999).

[6] L. Thrane, R.H. Jacobsen, P. Uhd Jepsen, and S.R. Keiding, *Chemical Physics Letters* **240** 330-333 (1995).

[7] A. Leitenstorfer, S. Hunsche, J. Shah, M.C. Nuss, and W.H. Knox, *Applied Physics Letters* **74** 1516-1518 (1999).